Plasma Deposition of Antibacterial Nano-coatings on Polymeric Materials.

A. Nikiforov[a], Ch. Leys[a], I. Kuchakova[a], M. Vanneste[b], P. Heyse[b], M. De Vrieze[b], A. Zille[c], Gh. Dinescu[d], B. Mitu[d], M. Modic[e], U. Cvelbar[e]

[a] Ghent University, Sint-Pietersnieuwstraat 41, 9000, Belgium
[b] CENTEXBEL, Technologiepark 7, BE-9052 ZWIJNAARDE, Belgium
[c] 2C2T - Centre for Textile Science and Technology, University of Minho, Campus de Azurém, 4800-058 Guimarães, Portugal
[d] National Institute for Lasers, Plasma and Radiation Physics and Faculty of Physics, University of Bucharest, IO7
[e] Jozef Stefan Institute, Jamova Cesta 39, Ljubljana 1000, Slovenia

Non-woven textile materials with antimicrobial properties are of high demands for applications ranging from medical dressing to everyday cleaning products. A plasma assisted route to engineer antimicrobial nano-composite coatings is proposed. Nano-particles of Ag, Cu and ZnO are tested as antimicrobial agents with average nano-particle size of 20-50 nm. Nanoparticles are incorporated in between two layers of an organosilicon film. The effect of the barrier coating on nano-particles release is determined by XPS. Antibacterial efficiency of the samples against *P. aeruginosa ATCC 9027* and *S. aureus M u50* bacteria shows that all treated samples exhibit higher antibacterial efficiency against *S. aureus*. The antibacterial efficiency of AgNPs and CuNPs is above 90% which is practically interesting for medical application while ZnONPs shows lower antibacterial efficiency.

Introduction

Industrial demands for materials with antibacterial coatings are intensively growing during last decade. The total value of the market is estimated to be as high as 1.6 billion USD. One of most promising areas of antibacterial materials applications is hospital use and health care. As biomedical devices and materials becoming an essential part of the human healthcare system, infections associated with the medical devices, especially with medical tools and supporting parts are responsible for at least 1.5% to 7.2% post-operational complications depending on the type of operational procedure [1, 2]. This poses significant health risk for patients and increased health costs through prolonged treatments. Moreover, due to the widespread use of biocides, prevalent antibacterial resistance has been developed [3, 4] often requiring new type of antibacterial materials. The earliest and essential event in the pathogenesis of an infection related to biomaterials is bacterial adhesion to them, formation of a biofilm that eventually leads to infection. A promising strategy to overcome the barrier is the fabrication of biomaterials with proper antimicrobial surfaces and controllable antibacterial effect, such as surfaces with designed micropatterns [5, 6], surfaces with attached chemical groups [7, 8], and surfaces with coatings incorporating antibiotics via novel physical and/or chemical methods [9-11].

Metal compounds like Ag (and salts) or Cu (and salts) are well known for their intrinsic antimicrobial property and the release of metal ions is believed to be the main reason for their antibacterial activity [12]. Solvated ions Ag^+, Cu^{2+} and others are highly active: they bind to tissue proteins and bring structural changes in the bacterial cell wall and DNA leading to cell distortion and death [13]. Among them Ag is the most investigated one. Due to their large surface-to-volume ratio and small size, silver nanoparticles (AgNPs) have merged up as a new generation of antibacterial with diverse medical applications [14]. Unfortunately, the emergence of cytotoxicity and genotoxicity of silver nanoparticles goes against some practical applications in human body [15-17]. Considering above concerns, it is important to fabricate a new class of antibacterial surfaces with firmly loading of AgNPs (or other nano-materials) and with precise release of antibacterial constituent from the materials. In this way, the release of nanoparticles to the microenvironment is limited and only silver ions are released locally. The world leading strategy is considered to be deposition of thin layer of antibacterial coatings on top surface of materials, like non-woven, fabrics and plastics (bandages, material of catheters, wound textile, medical masks, etc.) so that only surface of the materials will change and bulk properties are not affected.

Anchoring or grafting AgNPs on the topmost surface of substrates using wet chemical solution reactions have been discussed to enhance the efficiency of incorporation. In general, chemical pretreatment of substrates is implemented in order to introduce chemical groups such as amine group [18, 19] or sulfonated groups [20]. Then, substrates are immersed into a solution (typically $AgNO_3$, sodium citrate and $NaBH_4$) to exert the synthesis and grafts of AgNPs to the surface. However, the low concentration of silver (typically less than 2%) and weak bonds for the immobilization of AgNPs would affect the antibacterial efficiency.

The most promising technology for deposition of nanocomposite coating on industrial scale is the plasma assistant polymerization and sputtering. Recently, nanocomposite thin films composed of silver nanoparticles in a organosilicon polymer and a hydrocarbon matrix, have been deposited by associating plasma polymerization and silver sputtering within a low vacuum systems, using hexamethyldisiloxane and CO_2/C_2H_4 as precursor, respectively [21, 22]. The content of silver, controlled from the balance between the sputtering and polymerization, ranges from very few percentage to 29%. Unfortunately, the used technique has the limitation of treated samples size due to electrodes spacing, low deposition rate of some nm/min and high costs that definitely limits industrial application of the method. Therefore, it would be of significant interest to industry to fabricate nanocomposite thin films at sub-atmospheric and atmospheric pressure combining low energy costs of the process with efficiency of chemical methods and with films quality achieved only by low pressure plasma sputtering. In this work a new generation of coatings is proposed based on plasma of relatively high pressure with direct embedding of nanoparticles into coatings. Recently, a new kind of bimetallic/polymer nanocomposites so called "sandwich structures" were developed showing promising properties in the silver ion release studies [23, 24]. The principle behind the control of Ag ions release is the use of two layer coatings where first antibacterial nano-composite layer is covered by 5-50 nm thick second layer in order to tune coating performance to desirable efficiency and to prolong antibacterial effect of the material. Such kind of novel coatings is of great interest for medical applications and are tested in current work.

Experimental set-up

Deposition of the antibacterial coatings is carried out on non-woven polyethylene terephthalate (PET) fabrics. As a plasma source, low temperature discharges sustained by radio-frequency, direct current (DC) and AC voltage are tested in current work. All sources are characterized by low gas temperature below 50 ^{0}C that allows using them for deposition on heat sensitive polymers. In tests with 3 difference sources, a similar procedure has been used. For simplicity only the process of deposition with DC plasma jet is described below. Nano-particle composite coatings are prepared using a three step procedure as shown in Figure 1. An atmospheric pressure DC plasma jet, which consists of a pin-to-mesh electrode in a quartz tube, is used as the plasma source. The pin cathode, which is manufactured from a 2 mm tungsten rod with a conically sharpened tip, is connected to the negative polarity of a direct current high voltage power supply (Technix SR, France) through a ballast resistor. The mesh, 10mm away from the pin, is placed at the outlet of the tube. The substrate is placed 10mm away from the nozzle of the jet. By passing nitrogen through a bubble system, the organosilicon precursor HMDSO is vaporized. In order to prevent possible formation of microparticles in the gas phase, the diluting gas for the precursor is limited to 40 sccm (standard cubic centimeter per minute). Oxygen at 100 sccm is added to promote the conversion of the monomer. The first deposited layer of 70-200 nm is used as a reservation layer for the nanoparticles immobilization and control of the nanoparticles adhesion to the PET fabrics. Then, the samples with plasma deposited layer are immersed into a suspension of corresponding nanoparticles in ethanol and raised for drying. In number of experiments impregnation step has been replaced by use of aerosol of NPs of the same concentration as one used in impregnation procedure. In the final step, a second layer of organosilicon film with a thickness of 10-50 nm is deposited. This layer is used as a barrier to prevent the release of nanoparticles into the liquid medium. In this work, three different types of nanoparticles, silver nanoparticles (SSNANO, USA) of 20 nm size, zinc oxide nanoparticles (Sigma-Aldrich, Belgium) of 50 nm size and copper nanoparticles (Sigma-Aldrich, Belgium) of 50 nm size are used in the experiments as purchased for the preparation of corresponding nanocomposite fabrics.
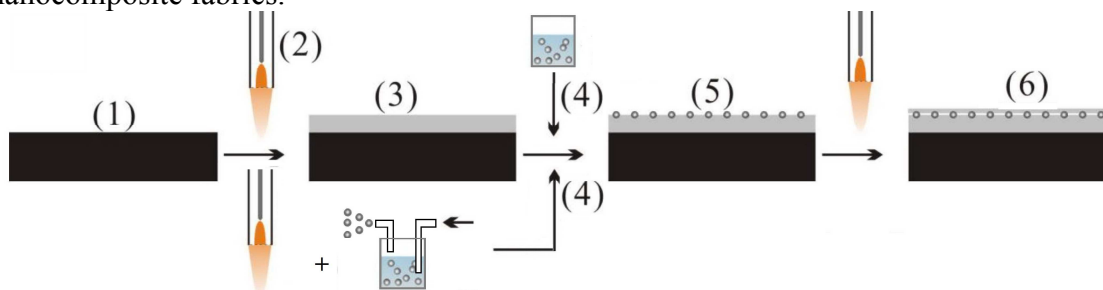

Figure 1. Scheme of the fabrication process: (1) raw non-woven PET fabric; (2) plasma jet deposition system; (3) deposition of the 1st layer (reservation layer); (4) nanoparticle dispersion; (5) nanoparticle incorporation on the surface; (6) deposition of the 2nd layer (barrier layer).

X-ray photoelectron spectroscopy (XPS) for surface characterization of deposited films is performed on a Versaprobe II system (Physical Electronics (PHI), USA) equipped with a monochromatic Al Kα X-ray source (hν = 1486.6 eV). The power of this source is set to 23.3 W. The pressure in the analyzing chamber is maintained below 10^{-7} Pa during analysis and the diameter of the analyzed area is 100 μm. Survey (0-1100 eV) and high

resolution spectra are recorded at a pass energy of 117.4 eV and 29.35 eV respectively. XPS analyses are performed with a take-off angle of 45° relatively to the sample surface. The value of 285 eV of the hydrocarbon C1s core level is used as a calibration of the energy scale.

Results and discussion

The first reservation layer deposited on the sample is used for increasing the load of NPs on the surface. It is found that at low ratio of the precursor HMDSO to O_2 in the mixture (10:90 ratio HMDSO/O_2, total N_2 flow 7000 sccm) the coatings are uniform and smooth. However increase of the ratio to 50:50 and even more to 90:10 results in formation of complex morphology of the deposits with very well developed surface. Typical morphology of the first layer deposited in nitrogen jet for different amount of precursor is presented on Figure 2.
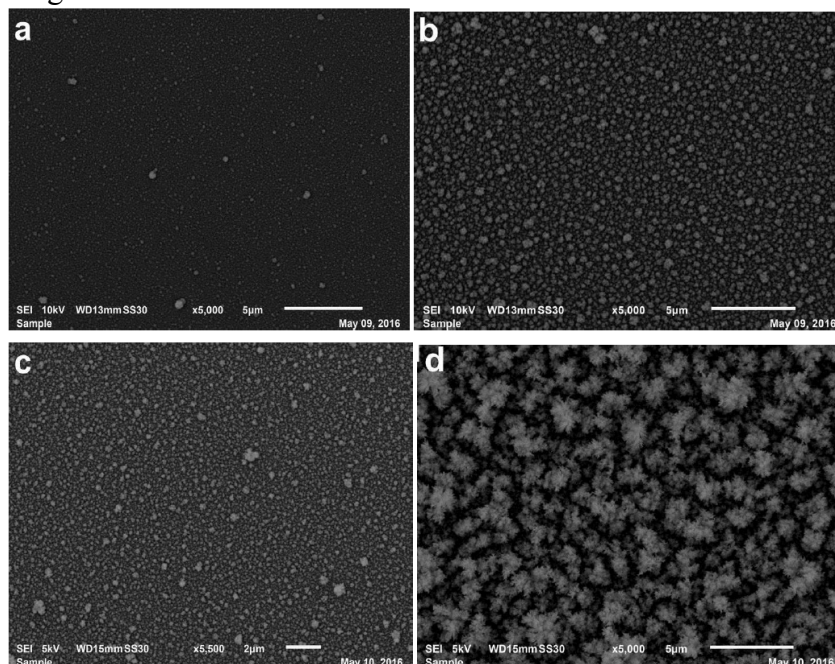

Figure 2. SEM images of deposited organosilicon film for different ratio of the precursor to oxygen at total flow rate of 7 l/min. For simplicity of analysis the deposition is carried out on a flat sample. Precursor/O_2 ratio: a) 10/90, b)10/50, c) 10/20, d)10/10

Indeed independent AFM tests of the coating surface have shown very high roughness of the coatings deposited at high ratio of precursor to oxygen as shown on Figure 3.
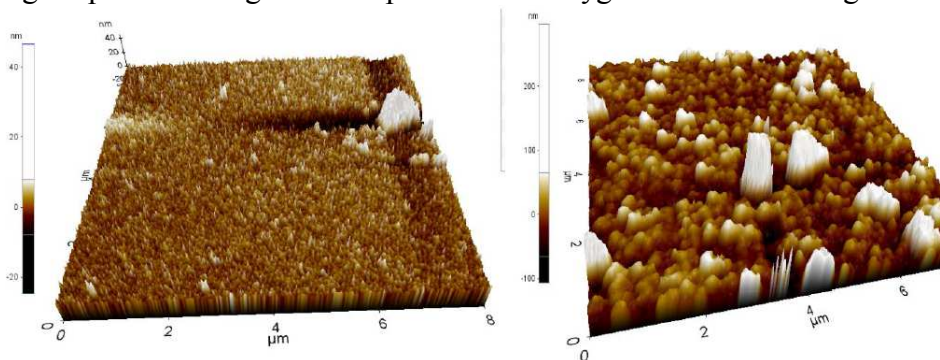

Figure 3. AFM images of organosilicon thin film deposited on flat substrate. Left image is obtained for ratio 10:90 and right side for a ratio 10:50.

It clearly indicates that preferable condition of the reservation layer deposition is a high ratio of the precursor to oxygen as it gives very developed 3D surface that allows high load of NPs into the reservation layer.

Load of the NPs inside of the coatings has been tested by both FTIR and XPS measurements. FTIR method itself does not give the possibility to quantify directly the content of NPs in the coatings. However, it demonstrates capability of plasma deposition process to incorporate substantial amount of NPs in the film. An example of FTIR spectrum obtained for composite with load of AgNPs in RF plasma jet is shown in Figure 4. Attribution of different peaks is demonstrated in Table 1.
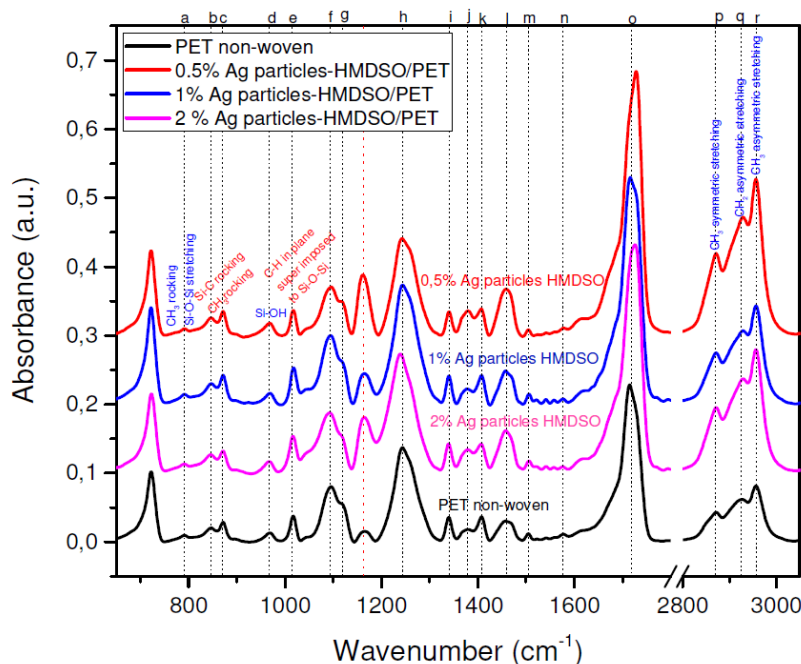

Figure 4. FTIR spectrum of coatings on non-woven PET fabrics deposited in RF plasma at atmospheric pressure and loaded with different amount of AgNPs. Attribution of different peaks is indicated in the figure as well in Table 1.

It is obvious from Figure 4 that specific chemical bonds for polymerized HMDSO materials are evident on non-woven PET fabrics. The presence of HMDSO barrier for the Ag-polysiloxane composite is revealed by increasing of FTIR absorbance signal and the FTIR signal increasing is more pronounced for higher content silver nanoparticles.

Figure 5 (b) – (d) displays the XPS high resolution spectra of silver, copper and zinc for those samples with corresponding nanoparticles. XPS method provides possibility of direct detection of NPs on the surface of the coatings. In Figure 5 (b), peaks at 368.2 eV and 374.2 eV are assigned to Ag 3d5/2 and Ag 3d3/2, respectively. These peaks have a splitting of 3d doublet with 6 eV indicating the presence of metallic silver. While, comparing to the binding energy of Ag 3d5/2 for bulk metal Ag at 368.2 eV, a positive chemical shift observed for Ag 3d5/2 (at 368.1 eV) suggests that silver nanoparticles are partly oxidized in the process. The Cu 2p1/2 and Cu 2p3/2 (Figure 5 (c)) centered at 952.2 eV and 932.4 eV with a spin-orbit separation of 18.8 eV for the sample embedding Cu-NPs. The absent of shake-up peaks at about 941.5 eV indicates no Cu^{2+} are presented in the sample. However, it is difficult to identify CuO and Cu^+ due to

the limitation of XPS resolution. Figure 5(d) represents the XPS spectra of Zn 2p, and the peak position of Zn 2p1/2 and Zn 2p3/2 locate at 1045.2 eV and 1022.2 eV, respectively.
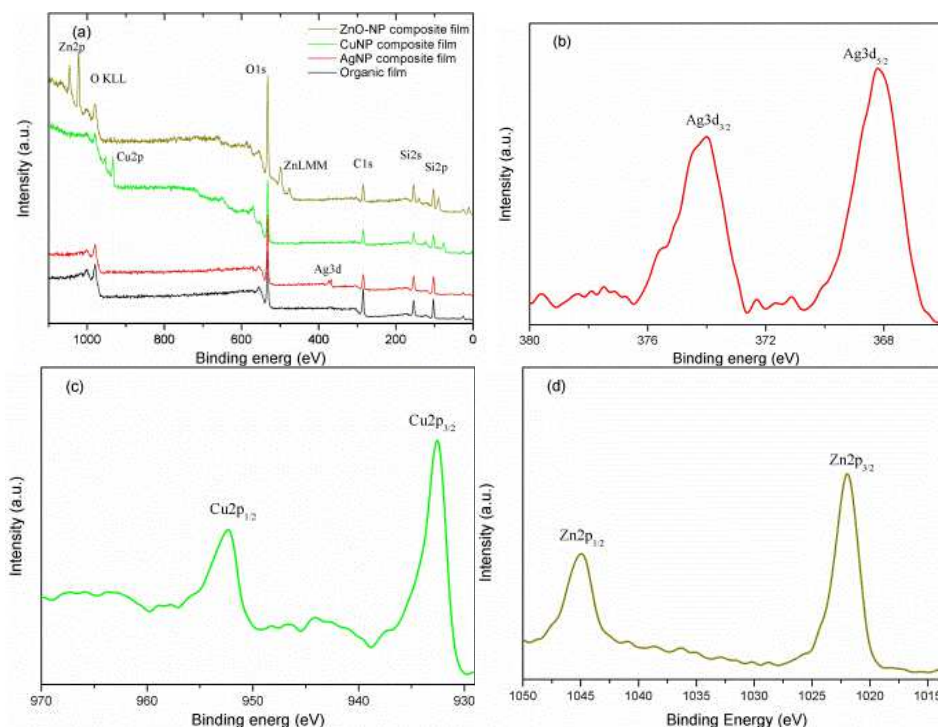

Figure 5. XPS results of the nanocomposite films: (a) survey XPS spectra; (b) Ag3d XPS spectrum; (c) Cu2p spectrum; (d) Zn2p spectrum. Deposition is carried out in DC jet working in nitrogen with NPs load of 1 mg/ml.

TABLE I. Attribution of different IR peaks in spectrum of the coatings to chemical bonds.

Position	Wavenumber (cm^{-1})	Chemical bond
a	790	CH3 rocking vibration and Si – O – Si, stretching vibration
b	847	Si – C rocking vibration and CH3; rocking vibration
c	871	C - H out of plane deformation
d	971	Si – OH bending vibration
e	1020	C - H in plane vibration super; imposed to Si – O – Si stretching vibration
f	1096	C – H in plane vibration
g	1120	C - O - C stretching vibration
h	1244	CH3 deformation vibration
i	1340	CH-wagging vibration, superimposed to O-H in plane deformation
j	1409	Triple skeletal aromatic vibrations
k	1455	CH2 scissoring vibration
l	1470	CH2 scissoring
m	1505	Triple skeletal aromatic vibrations
n	1576	Triple skeletal aromatic vibrations
o	1712	C=O bending vibration
p	2870	CH3 symmetric stretching
q	2907	CH2 asymmetric stretching
r	2958	CH3 asymmetric stretching

It has to be noted that considerable change in XPS spectra and morphology of the coatings has been observed for samples prepared with preliminary sonification of the NPs in solution for 20 minutes and without sonification step. It is well known that NPs can strongly agglomerate in relatively short time of seconds/minutes that results in significant decrease of their antibacterial activity. Effect of sonification step on deposition is shown in Figure 6.
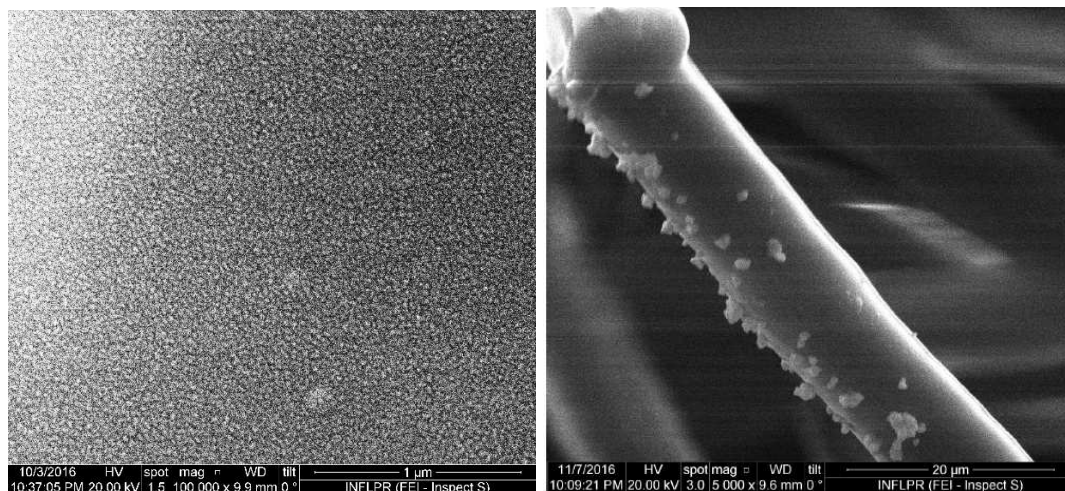

Figure 6. SEM images of non-woven fabrics with AgNPs composite coating obtained by RF discharge deposition (left) with preliminary sonification and visible NPs; (right) without sonification step.

On Figure 6 one can clearly see NPs deposited and well distributed on the surface of the fibres if the sonification is applied. However, no NPs are distinguishable in case of coatings obtained without sonification and only large clusters of NPs are visible on surface of the fibres. It has to be noted that formation of agglomerates of NPs should strongly affects ion release from NPs surface and such an aggregation has to be avoided whenever it is possible. To this end all the samples tested in the following part of the work for antibacterial activity have been prepared with sonification of NPs solution.

The antimicrobial properties of the samples prepared with different load, different kind of NPs and different thickness of the barrier layer were tested against P. aeruginosa and S. aureus. Initial sample with a 70 nm organosilicon reservation film having no antimicrobial activity was used as a control. Antimicrobial capability of the treated PET fabrics with a 25 nm and 50 nm barrier layer, corresponding to scanning velocity of 1 and 0.5 mm/sec is shown in Figure 7.
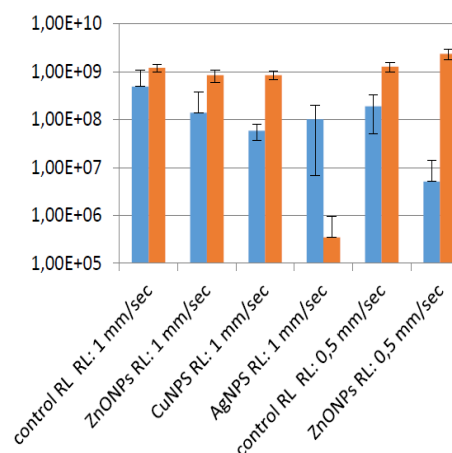
Figure 7. Antibacterial effect of different coatings obtained through deposition with scanning of the surface at different velocity 0.5 and 1 mm/s corresponding to 50 and 25 nm barrier layer thickness. Blue color – S. aureus Mu50, red color – P.aeruginossa ATCC9027

All the samples with AgNPs exhibit antimicrobial activity against both microorganisms, which clearly indicated that the growth of microorganisms in medium was affected by the presence of AgNPs. Treated PET fabrics show higher efficiency against S. aureus and lower against P. aeruginosa, which is in agreement with the results on commercially available silver-containing dresses. The samples with AgNPs without a barrier layer have shown highest reduction of more than 90% of S. aureus and 80% of P. aeruginosa. Presence of the barrier layer results in a decrease of the antimicrobial efficiency to almost 50% reduction in the case of a 50 nm barrier layer. Such a strong effect of the barrier layer can be linked to the way how AgNPs induce the antimicrobial effect. Similar trends are observed for CuNPs as for AgNPs that indicates that CuNPs can be a good alternative to expensive silver. ZnO particles were less effective against both bacteria as an antibacterial mechanism of ZnO is considerably different from Cu and Ag and usually UV light is required for ZnO activation.

Conclusions

An approach for deposition of antibacterial coatings on non-woven fabrics is tested. Three different sources of plasma are used for deposition. It is demonstrated that despite different methods of plasma sustaining all the sources are capable of deposition multilayer antibacterial coatings. Non-woven fabrics incorporated with three types of nanoparticles - AgNP, CuNP and ZnONP - have been prepared by atmospheric pressure plasma process. Load of NPs from 10 μg/ml to 20 mg/ml (in solution) has been used to incorporate different amount of NPs in the coatings whereas thickness of the barrier layer has been used to control release of antibacterial agent. The XPS results reveal that the nanoparticles have been successfully embedded into the fabrics. All materials show effective antibacterial activity against *S. aureus* and *P.aeruginossa*. It is found that use of CuNPs has almost the same efficiency as AgNPs, whereas ZnONPs demonstrated lower efficiency against *S. aureus* and *P.aeruginossa*. The results prove that the methods for the immobilization of nanoparticles in to the structure of non-woven fabrics might present a new route for preparation of highly effective antibacterial materials for future applications.

Acknowledgments

References

1. J. K. Parsons, I. Varkarakis, K. H. Rha, T. W. Jarrett, P. A. Pinto, L. R. Kavoussi, *Urology.*, **63**, 27 (2004).
2. K. Ogura, H. Yasunaga, H. Horiguchi, K. Ohe, Y. Shinoda, S. Tanaka, H. Kawano, *J. Bone Joint Surg. Am.*, **95**, 1684 (2013).
3. Grainger DW, van der Mei HC, Jutte PC, van den Dungen JJAM, Schultz MJ, van der Laan BFAM, et al. *Biomaterials*, **34**(37), 9237-43 (2013).
4. Levy SB, Marshall B. *Nat Med.*, **10**, 122-9 (2004).
5. Arias CA, Murray BE. *New Engl J Med.*, **360**(5), 439-43 (2009).
6. Singh AV, Vyas V, Patil R, Sharma V, Scopelliti PE, Bongiorno G, et al. *Plos One*, **6**(9), e25029 (2011).
7. Anselme K, Davidson P, Popa A, Giazzon M, Liley M, Ploux L. *Acta Biomaterialia,* **6**(10), 3824-46 (2010).
8. Banerjee I, Pangule RC, Kane RS. *Advanced Materials*, **23**(6), 690-718 (2011).
9. Kerkeni A, Behary N, Dhulster P, Chihib NE, Perwuelz A. *J Appl Polym Sci.*, **129**(2), 866-73 (2013).
10. Taglietti A, Arciola CR, D'Agostino A, Dacarro G, Montanaro L, Campoccia D, et al. *Biomaterials*, **35**(6), 1779-88 (2014).
11. Garcia-Fernandez MJ, Martinez-Calvo L, Ruiz JC, Wertheimer MR, Concheiro A, Alvarez-Lorenzo C. *Plasma Process Polym.*, **9**(5), 540-9 (2012).
12. Braceras I, Oyarbide J, Azpiroz P, Briz N, Ipinazar E, Alvarez N, et al. *Plasma Process Polym.*, **10**(4), 328-35 (2013).
13. Hasan J, Crawford RJ, Ivanova EP. *Trends Biotechnol.*, **31**(5), 295-304 (2013)
14. Feng Q, Wu J, Chen G, Cui F, Kim T, Kim J. *J Biomed Mater Res.*, **52**(4), 662-8 (2000).
15. Marambio-Jones C, Hoek EMV. *J Nanopart Res.*, **12**(5), 1531-51 (2010).
16. Rai M, Yadav A, Gade A. *Biotechnol Adv.*, **27**(1), 76-83 (2009).
17. Chaloupka K, Malam Y, Seifalian AM. *Trends Biotechnol.*, **28**(11), 580-8 (2010).
18. AshaRani P, Low Kah Mun G, Hande MP, Valiyaveettil S. *Acs Nano*, **3**(2), 279-90 (2008).
19. Carlson C, Hussain S, Schrand A, K. Braydich-Stolle L, Hess K, Jones R, et al.. *J Phys Chem B.*, **112**(43), 13608-19 (2008).
20. AshaRani PV, Hande MP, Valiyaveettil S. *BMC Cell Biol.*, **10** (2009).
21. Ferrer MCC, Hickok NJ, Eckmann DM, *Soft Matter.*, **8**(8), 2423-31 (2012).
22. Cao X, Tang M, Liu F, Nie Y, Zhao C. Colloids Surf B, **81**(2), 555-62 (2010).
23. V. Zaporojtchenko, R. Podschun, U. Schürmann, A. Kulkarni, and F. Faupel, Nanotechnology, **17**, 19 4904-4908 (2006).
24. N. Alissawi, et al., Journal of Nanoparticle Research, **14**, 7 928-939 (2012).